

**Cell Reports, Volume 26**

**Supplemental Information**

**Vectorial Import via a Metastable Disulfide-Linked  
Complex Allows for a Quality Control Step and  
Import by the Mitochondrial Disulfide Relay**

**Markus Habich, Silja Lucia Salscheider, Lena Maria Murschall, Michaela Nicole Hoehne, Manuel Fischer, Fabian Schorn, Carmelina Petrunaro, Muna Ali, Alican J. Erdogan, Shadi Abou-Eid, Hamid Kashkar, Joern Dengjel, and Jan Riemer**

## SUPPLEMENTAL TABLES

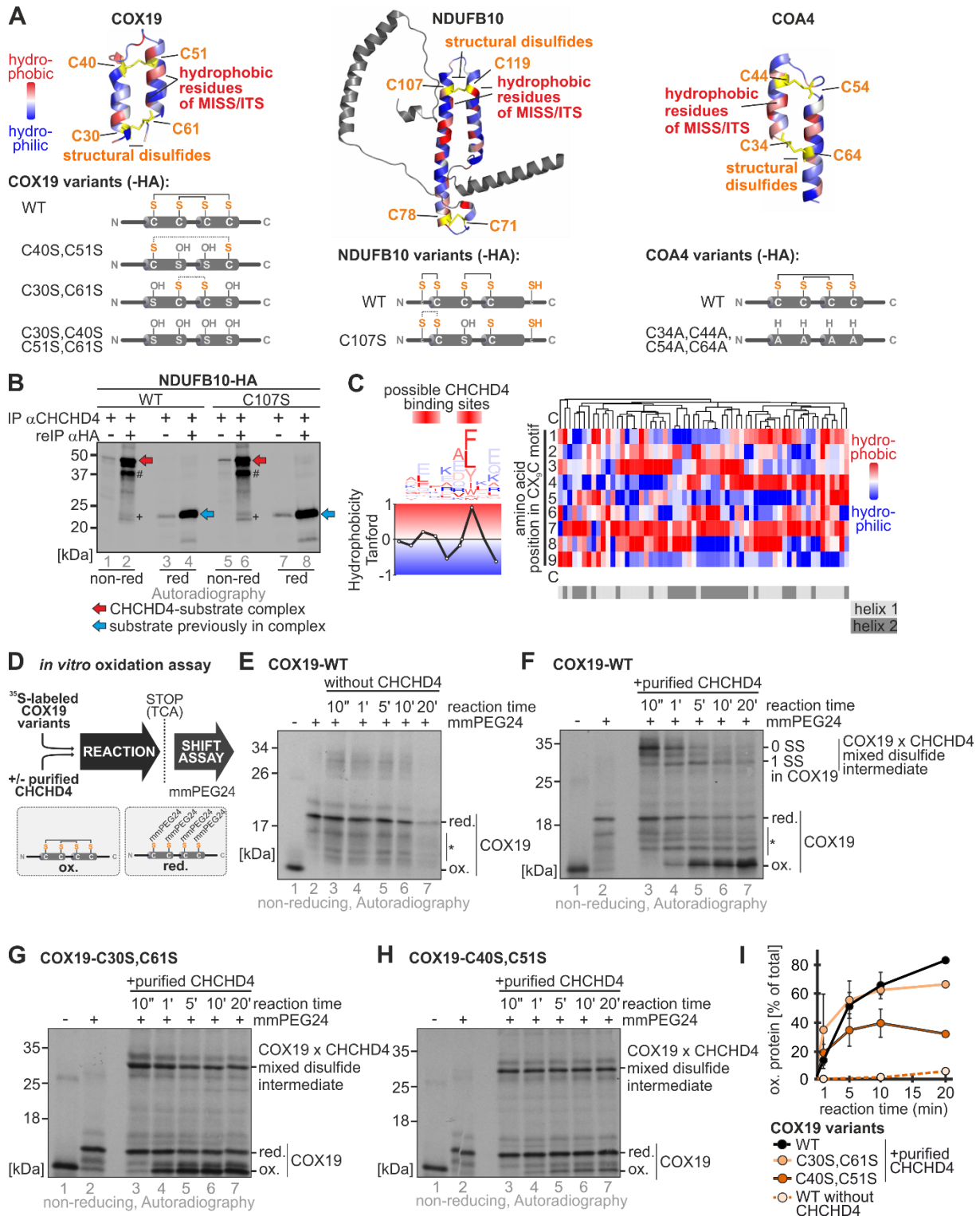
**Table S1:** Proteomic data: Refer to enclosed Excel file, Related to Figure 3

**Table S2:** Plasmids and cell lines used in this study, Related to Star methods:

Cell line	Plasmid	Gene	Tag (C-terminal)	Reference
Flp-In T-REx-293-Mock	pcDNA5/FRT/TO	--	--	Fischer et al., 2013
Flp-In T-REx-293-COX19	pcDNA5/FRT/TO	ORF <i>COX19</i>	HA	Fischer et al., 2013
Flp-In T-REx-293-COX19 C30,C61S	pcDNA5/FRT/TO	ORF <i>COX19</i> ( <i>G</i> <sub>89</sub> ► <i>C</i> ; <i>G</i> <sub>182</sub> ► <i>C</i> )	HA	this study
Flp-In T-REx-293-COX19 C40,C51S	pcDNA5/FRT/TO	ORF <i>COX19</i> ( <i>G</i> <sub>119</sub> ► <i>C</i> ; <i>G</i> <sub>152</sub> ► <i>C</i> )	HA	this study
Flp-In T-REx-293-COX19 C30,C40S,C51S,C61S	pcDNA5/FRT/TO	ORF <i>COX19</i> ( <i>G</i> <sub>89</sub> ► <i>C</i> ; <i>G</i> <sub>119</sub> ► <i>C</i> ; <i>G</i> <sub>152</sub> ► <i>C</i> ; <i>G</i> <sub>182</sub> ► <i>C</i> )	HA	this study
Flp-In T-REx-293-COA4	pcDNA5/FRT/TO	ORF <i>COA4</i>	HA	Fischer et al., 2013
Flp-In T-REx-293-COA4 C34A,C44A,C54A,C64A	pcDNA5/FRT/TO	ORF <i>COA4</i> ( <i>T</i> <sub>100</sub> ► <i>G</i> ; <i>G</i> <sub>101</sub> ► <i>C</i> ; <i>T</i> <sub>130</sub> ► <i>G</i> ; <i>G</i> <sub>131</sub> ► <i>C</i> ; <i>T</i> <sub>160</sub> ► <i>G</i> ; <i>G</i> <sub>161</sub> ► <i>C</i> ; <i>T</i> <sub>190</sub> ► <i>G</i> ; <i>G</i> <sub>191</sub> ► <i>C</i> )	HA	this study
Flp-In T-REx-293-CHCHD4	pcDNA5/FRT/TO	ORF <i>CHCHD4</i>	Strep	Fischer et al., 2013
Flp-In T-REx-293-CHCHD4 C53S	pcDNA5/FRT/TO	ORF <i>CHCHD4</i> ( <i>T</i> <sub>157</sub> ► <i>G</i> )	Strep	this study
Flp-In T-REx-293-CHCHD4 C55S	pcDNA5/FRT/TO	ORF <i>CHCHD4</i> ( <i>T</i> <sub>163</sub> ► <i>G</i> )	Strep	this study
Flp-In T-REx-293-CHCHD4 C53S,C55S	pcDNA5/FRT/TO	ORF <i>CHCHD4</i> ( <i>T</i> <sub>157</sub> ; <i>T</i> <sub>163</sub> ► <i>G</i> )	Strep	Fischer et al., 2013
Flp-In T-REx-293-CHCHD4 F68E	pcDNA5/FRT/TO	ORF <i>CHCHD4</i> ( <i>T</i> <sub>202</sub> ; <i>T</i> <sub>204</sub> ► <i>G</i> ; <i>T</i> <sub>203</sub> ► <i>A</i> )	Strep	this study
Flp-In T-REx-293-CHCHD4 C53S,C55S F68E	pcDNA5/FRT/TO	ORF <i>CHCHD4</i> ( <i>T</i> <sub>157</sub> ; <i>T</i> <sub>163</sub> ► <i>G</i> ; <i>T</i> <sub>202</sub> ; <i>T</i> <sub>204</sub> ► <i>G</i> ; <i>T</i> <sub>203</sub> ► <i>A</i> )	Strep	this study
Flp-In T-REx293-Smac MTS-COX19	pcDNA5/FRT/TO	ORF <i>SMAC</i> (bp 1-177), ORF <i>COX19</i>	HA	Fischer et al., 2013
Flp-In T-REx293-Smac MTS-COX19 C30,61S	pcDNA5/FRT/TO	ORF <i>SMAC</i> (bp 1-177), ORF <i>COX19</i> ( <i>G</i> <sub>89</sub> ► <i>C</i> ; <i>G</i> <sub>182</sub> ► <i>C</i> )	HA	this study
Flp-In T-REx293-Smac MTS-COX19 C40,51S	pcDNA5/FRT/TO	ORF <i>SMAC</i> (bp 1-177), ORF <i>COX19</i> ( <i>G</i> <sub>119</sub> ► <i>C</i> ; <i>G</i> <sub>152</sub> ► <i>C</i> )	HA	this study
Flp-In T-REx293-Smac MTS-COX19 C30,40,51,61S	pcDNA5/FRT/TO	ORF <i>SMAC</i> (bp 1-177), ORF <i>COX19</i> ( <i>G</i> <sub>89</sub> ► <i>C</i> ; <i>G</i> <sub>119</sub> ► <i>C</i> ; <i>G</i> <sub>152</sub> ► <i>C</i> ; <i>G</i> <sub>182</sub> ► <i>C</i> )	HA	this study
Flp-In T-REx293-NDUFB10	pcDNA5/FRT/TO	ORF <i>NDUFB10</i>	HA	this study
Flp-In T-REx293-NDUFB10 C107S	pcDNA5/FRT/TO	ORF <i>NDUFB10</i> <i>T</i> <sub>319</sub> ► <i>A</i>	HA	this study
Flp-In T-REx293-cytochrome <i>b</i> <sub>2</sub> MTS-GRX1	pcDNA5/FRT/TO	ORF <i>S. cerevisiae</i> cytochrome <i>b</i> <sub>2</sub> (bp1-258), ORF <i>H. sapiens</i> GRX1	roGFP2	this study
HEK293T	--	--	--	this study
HEK293T CHCHD4 knockout #2	pSpCas9(BB)-2A-GFP	Guide #2 FW: caccgCCTCATCCTCTTGGGGATAG RV: aaacCTATCCCCAAGAGGATGAGGc	--	this study
HEK293T CHCHD4 knockout #3	pSpCas9(BB)-2A-GFP	Guide #3 FW: caccgCCTCTATCCCCAAGAGGATG RV: aaacCATCCTCTTGGGGATAGAGGc	--	this study
HEK293T CHCHD4 knockout #2-Mock	PB-CuO-MCS-IRES-GFP-EF1-CymR-Puro	--	--	this study

HEK293T CHCHD4 knockout #2-CHCHD4	PB-CuO-MCS-IRES-GFP-EF1-CymR-Puro	ORF <i>CHCHD4</i>	--	this study
HEK293T CHCHD4 knockout #2-C53S	PB-CuO-MCS-IRES-GFP-EF1-CymR-Puro	ORF <i>CHCHD4</i> (T157►G)	--	this study
HEK293T CHCHD4 knockout #2-C53S, C55S	PB-CuO-MCS-IRES-GFP-EF1-CymR-Puro	ORF <i>CHCHD4</i> (T157; T163►G)	--	this study
HEK293T CHCHD4 knockout #2-CHCHD4 F68E	PB-CuO-MCS-IRES-GFP-EF1-CymR-Puro	ORF <i>CHCHD4</i> (T202;T204►G; T203►A)	--	this study
HEK293T CHCHD4 knockout #3-Mock	PB-CuO-MCS-IRES-GFP-EF1-CymR-Puro	--	--	this study
HEK293T CHCHD4 knockout #3-CHCHD4	PB-CuO-MCS-IRES-GFP-EF1-CymR-Puro	ORF <i>CHCHD4</i>	--	this study
HEK293T CHCHD4 knockout #3-C53S	PB-CuO-MCS-IRES-GFP-EF1-CymR-Puro	ORF <i>CHCHD4</i> (T157►G)	--	this study
HEK293T CHCHD4 knockout #3-C53S, C55S	PB-CuO-MCS-IRES-GFP-EF1-CymR-Puro	ORF <i>CHCHD4</i> (T157; T163►G)	--	this study
HEK293T CHCHD4 knockout #3-CHCHD4 F68E	PB-CuO-MCS-IRES-GFP-EF1-CymR-Puro	ORF <i>CHCHD4</i> (T202;T204►G; T203►A)	--	this study

## SUPPLEMENTAL FIGURES



**Supplementary Figure 1. CHCHD4 interacts with and oxidizes COX19 cysteine variants lacking the inner or the outer disulfide bond *in vitro* (related to Figure 1)**

**A)** Structure of COX19, NDUFB10 and COA4 as well as the respective mutated variants used in this study. The structure of human COX19 (Uniprot: Q49B96) was built on the solution structure of CHCHD7 (pdb: 2LQT) with SWISS-MODEL. The structure of human NDUFB10 (pdb: 5XTC). NDUFB10C107 represents a human disease mutant. The structure of human COA4 (Uniprot: Q9NYJ1) was built on the solution structure of CHCHD7 (pdb: 2LQT) with

SWISS-MODEL. Colour-coding represents hydrophobicity of the amino acids according to the Tanford hydrophobicity scale.

**B)** *In cell* CHCHD4-substrate interaction assay for NDUFB10 and a patient variant of the protein (NDUFB10<sup>C107S</sup>). Performed as described in Figure 1A. 1% of the IP against CHCHD4 was loaded as control. Expression was induced during the 20 min pulse with 1 µg/ml doxycycline. CHCHD4 interacts covalently with wildtype NDUFB10 and with the patient mutant NDUFB10<sup>C107S</sup> *in vivo*. *red*, reducing SDS-PAGE; *non-red*, non-reducing SDS-PAGE. *red arrow*, disulphide-linked CHCHD4-NDUFB10 dimer; *blue arrow*, NDUFB10. *hash tag*, disulphide-linked CHCHD4-NDUFB10 dimer possibly with truncated CHCHD4; *plus sign*, NDUFB10 not in disulphide-linked complex. (n=2 biological replicates)

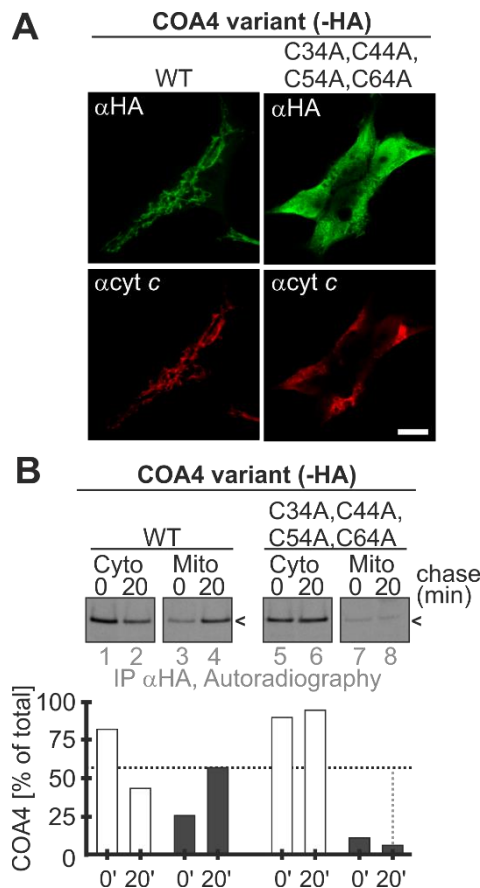
**C)** Twin CX<sub>9</sub>C proteins contain multiple potential CHCHD4 interaction sites. Amino acids in twin CX<sub>9</sub>C motifs were scored for hydrophobicity using the Tanford scale. Data was grouped using hierarchical clustering (metric: euclidean distance; linkage method: average) and plotted in a heatmap using Morpheus (<https://software.broadinstitute.org/morpheus/>). Both helices of most substrates (depicted in light and dark grey, respectively) are sufficiently amphipathic to allow initial hydrophobic interaction with CHCHD4 that is required for formation of the disulphide-linked metastable complex. This is also reflected by the overall hydrophobicity as outlined in the graph.

**D)** *In vitro* oxidation kinetics assay. Recombinant expressed and purified human CHCHD4 was added to <sup>35</sup>S-labeled COX19 variants to allow disulphide exchange reactions. The reaction was stopped by rapid acidification via addition of trichloroacetic acid (TCA). Lysates were treated with mmPEG24 to determine protein redox states, followed by SDS-PAGE and autoradiography. Reduced COX19 is modified with four mmPEG24, whereas oxidized COX19 remains unmodified.

**E)** Control experiment. Wildtype COX19 does not become oxidized in the absence of CHCHD4. Small amounts of *in vitro* translated radioactive COX19 were incubated with buffer for the indicated times, TCA-precipitated, and incubated with 15 mM mmPEG24 for 1 hr at 25°C. Protein was analysed by non-reducing SDS-PAGE and autoradiography. Reduced and oxidized forms as well as semi-oxidized intermediates (\*) of COX19 are indicated. (n=2 biological replicates)

**F-H)** Oxidation kinetics of COX19 cysteine variants. CHCHD4 oxidizes COX19 variants lacking the cysteines for the outer and inner disulphide bond, respectively. Performed as described in (D), except that *in vitro* translated radioactive COX19 was incubated with 30 µM purified CHCHD4 for the indicated times. Reduced and oxidized forms of COX19 as well as COX19-CHCHD4 complexes are indicated. Apparently, oxidation of COX19<sup>WT</sup> can follow two routes: 1) In the COX19<sup>WT</sup>-CHCHD4 complex, COX19 forms one disulphide bond over time and is then released as fully oxidized protein (two bands for the complex), 2) COX19 disulphide bonds are serially introduced. Occurrence of multiple semi-oxidized intermediates (\*) might indicate off-target intermediates that also appear to persist over the duration of the experiment. (n=2 biological replicates)

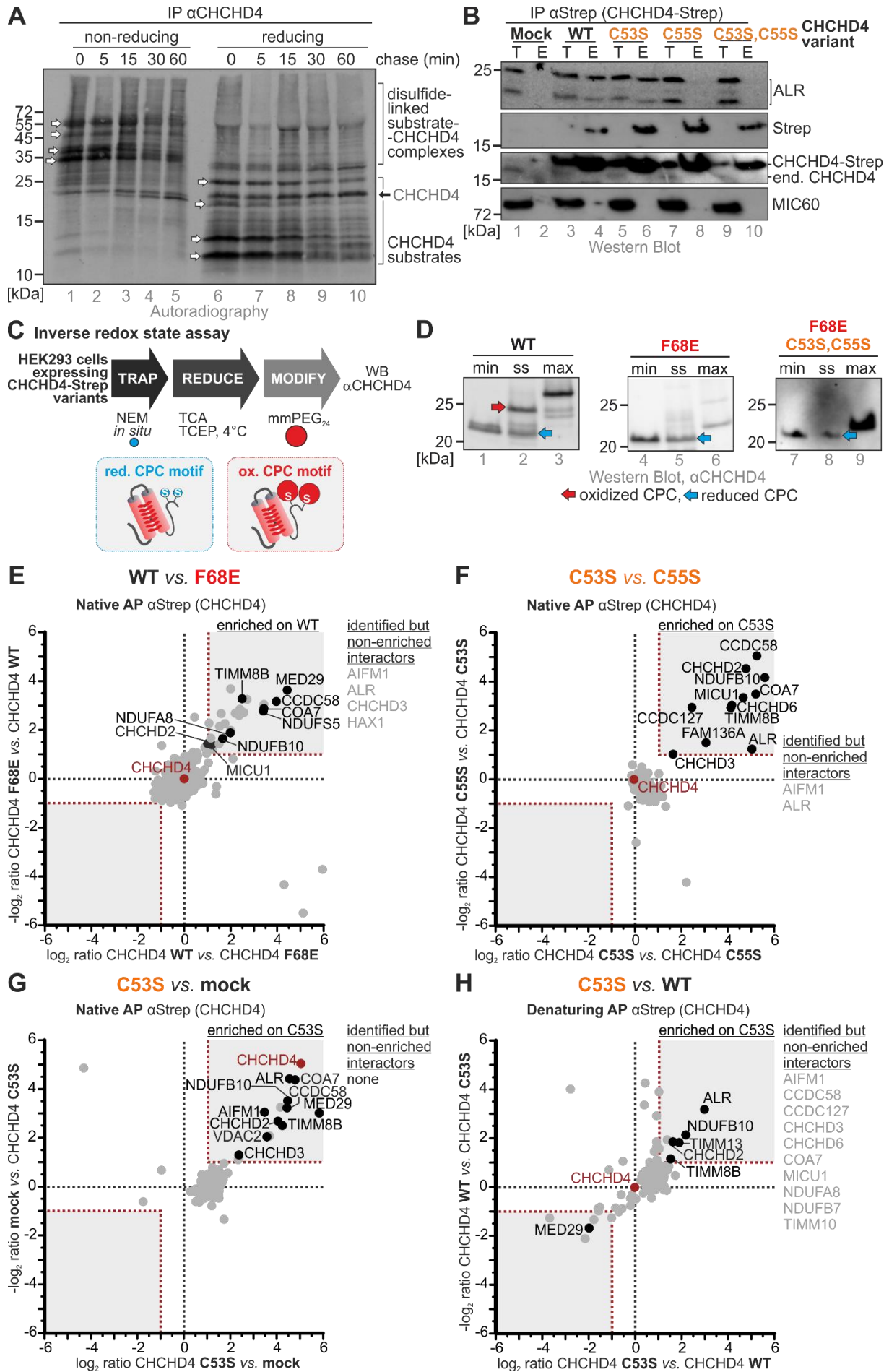
**I)** Quantification of (E) to (H) using ImageJ. Data from two experiments were combined.



**Supplementary Figure 2. COA4-HA cysteine variants do not accumulate in mitochondria.**  
(related to Figure 2)

**A)** Localization of COA4-HA cysteine variant.. HEK293 cells stably expressing the indicated COA4-HA variants were incubated for 24 hours with 1  $\mu$ g/ml doxycycline to induce expression. Cells were fixated, permeabilized and stained using primary antibodies against the HA epitope ( $\alpha$ HA; green) and cytochrome c ( $\alpha$ cyt c; red). Cells were analysed by fluorescence microscopy. While COA4<sup>WT</sup>-HA accumulated in mitochondria, the cysteine variant did not. Instead, it remained in the cytosol. Scale bar = 10  $\mu$ m. (WT: n=6 cells, C34A,C44A,C54A,C64A: n=10 cells, technical replicates)

**B)** Pulse chase fractionation experiment of COA4-HA cysteine variants expressed in HEK293 cells. Expression was induced by doxycycline treatment for one hour before the pulse chase experiment. Cells were first pulse labelled for 5 min with <sup>35</sup>S-methionine and then chased with cold methionine for 0 or 20 min. At the end of the chase, cells were transferred to ice and incubated with low concentration of digitonin for 10 min to selectively permeabilize the plasma membrane and leave the OMM intact. To separate the mitochondrial from the cytosolic fraction, lysates were centrifuged and COA4-HA was immunoprecipitated (IP). Eluates were analysed by SDS-PAGE and autoradiography. While COA4<sup>WT</sup>-HA accumulated in mitochondria, the cysteine variant did not. Instead, it remained in the cytosol. (n=2 biological replicates)



**Supplementary Figure 3. Parameters of CHCHD4-substrate and CHCHD4-ALR interaction** (related to Figure 3)

**A)** CHCHD4-substrate interaction is transient. HEK293 cells were pulse-labeled with <sup>35</sup>S-methionine for 1 hour. Then, thiol-exchange reactions were inhibited by addition of NEM to preserve mixed disulphides. Cells were lysed in 2% SDS. Then, lysates were subjected to IP against CHCHD4, analysed by non-reducing or reducing SDS-PAGE and autoradiography. Disulphide-linked substrate-CHCHD4 complexes and CHCHD4 substrates are indicated. (n=2 biological replicates)

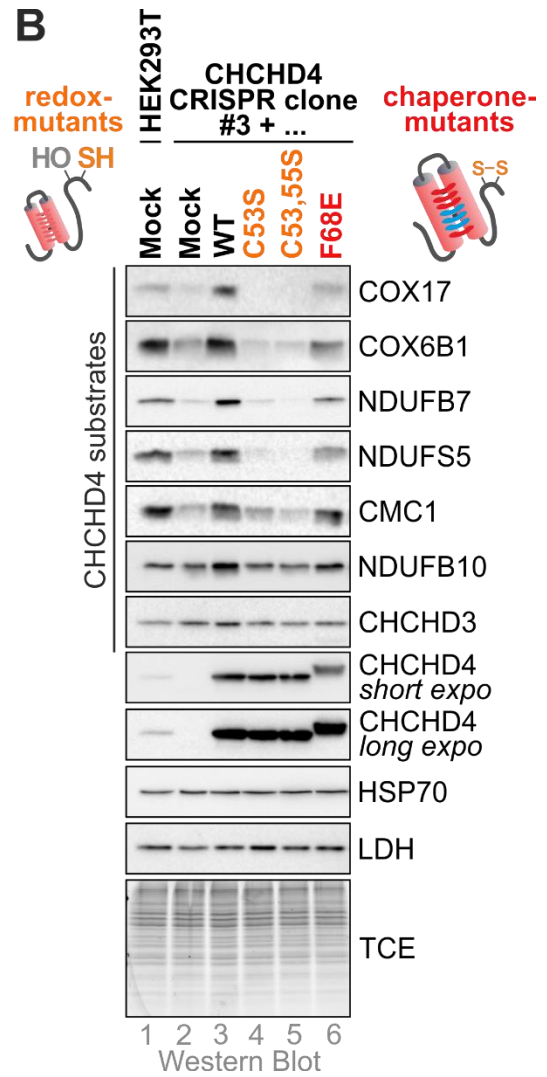
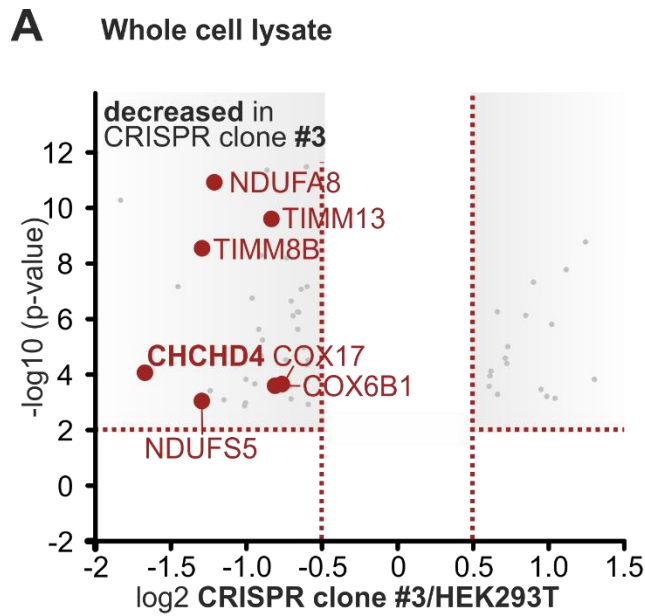
**B)** CHCHD4<sup>WT</sup> and CHCHD4<sup>C53S</sup> interact with ALR. HEK293 cells stably expressing different CHCHD4 cysteine variants were treated with NEM to block thiol-disulphide exchange. Then, denaturing IP against the Strep-tag was performed. Total sample (T) and eluates (E) were analysed by SDS-PAGE and immunoblot against the indicated proteins. (n=1)

**C)** Schematic inverse shift assay for the determination of the CHCHD4 redox state. To determine the redox state of CHCHD4 at steady state, intact cells were treated with NEM to stop all thiol-disulphide exchange reactions and trap the redox state of CHCHD4. Then, cells were lysed and lysates were treated at 4 °C with TCEP. Previously oxidized cysteines in the CPC motif are now accessible to modification with mmPEG24. As controls, unmodified samples (min) and samples without NEM pretreatment (max) were loaded.

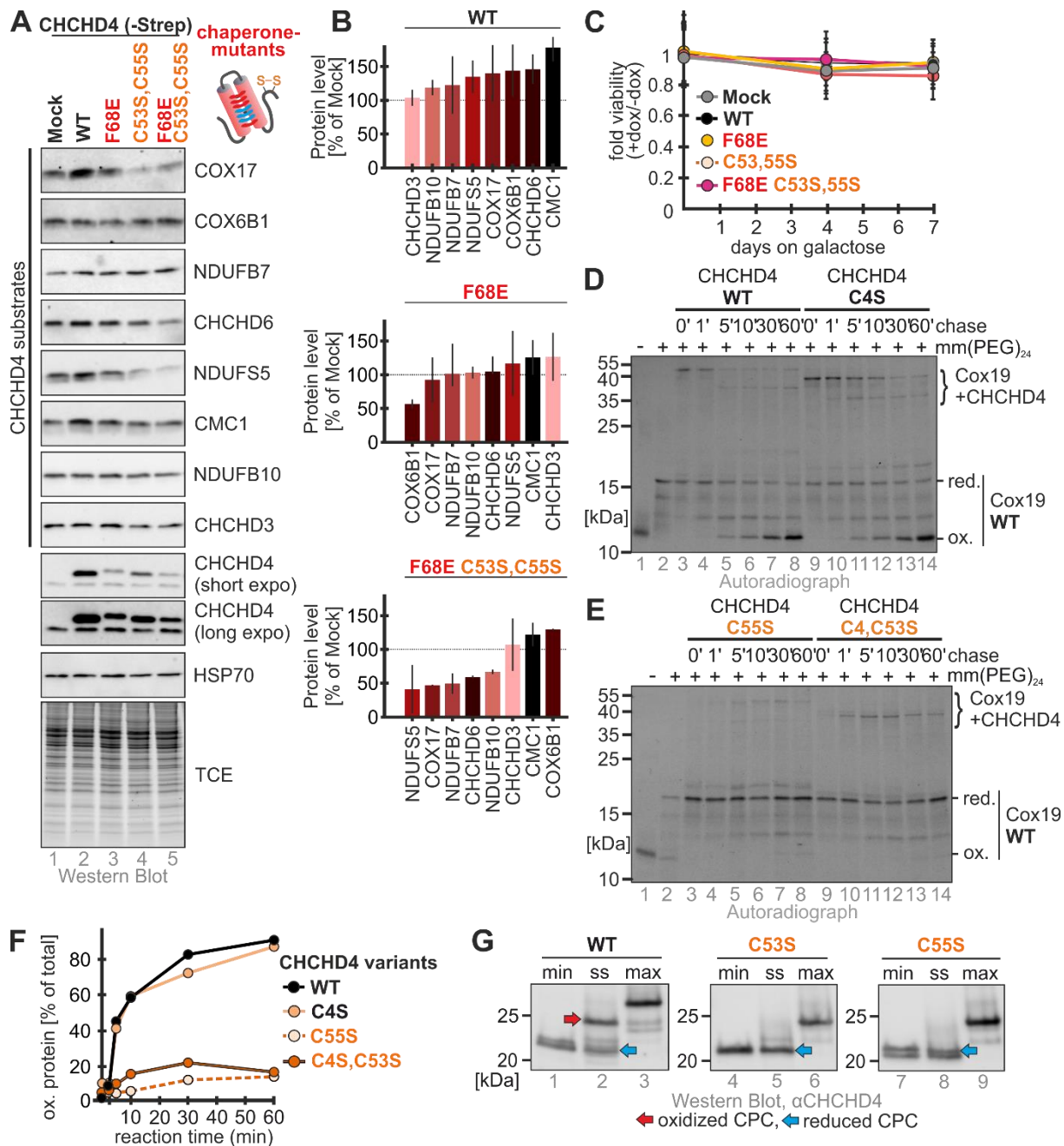
**D)** Redox state of F68E variants of CHCHD4. These variants are almost completely reduced at steady state. Performed as described in (C). (n=2 biological replicates)

**E-H)** Interaction partners of CHCHD4 cysteine variants and the F68E mutant from native and denaturing affinity purification (AP). Cells were grown in SILAC medium. Cells were treated with NEM, mixed and lysed under native or denaturing conditions. CHCHD4-Strep variants were enriched using strep-tactin beads and eluates were analysed by mass spectrometry. The experiment was reproduced with inverted isotope labelling. Results from both experiments are plotted against each other. Proteins were counted as hits if at least two peptides per protein were enriched more than 2-fold. (n=2 biological replicates)





**Supplementary Figure 4. Reproduction of data shown in Figure 4 with a second CRISPR clone.** (related to Figure 4). Findings obtained with clone #3 are analogues to data obtained with clone #2 (Figure 4) (A: n=3 biological replicates, B: n=2 biological replicates)



**Supplementary Figure 5. Properties of ‘redox’ and ‘chaperone’ mutants of CHCHD4.** (related to Figure 5)

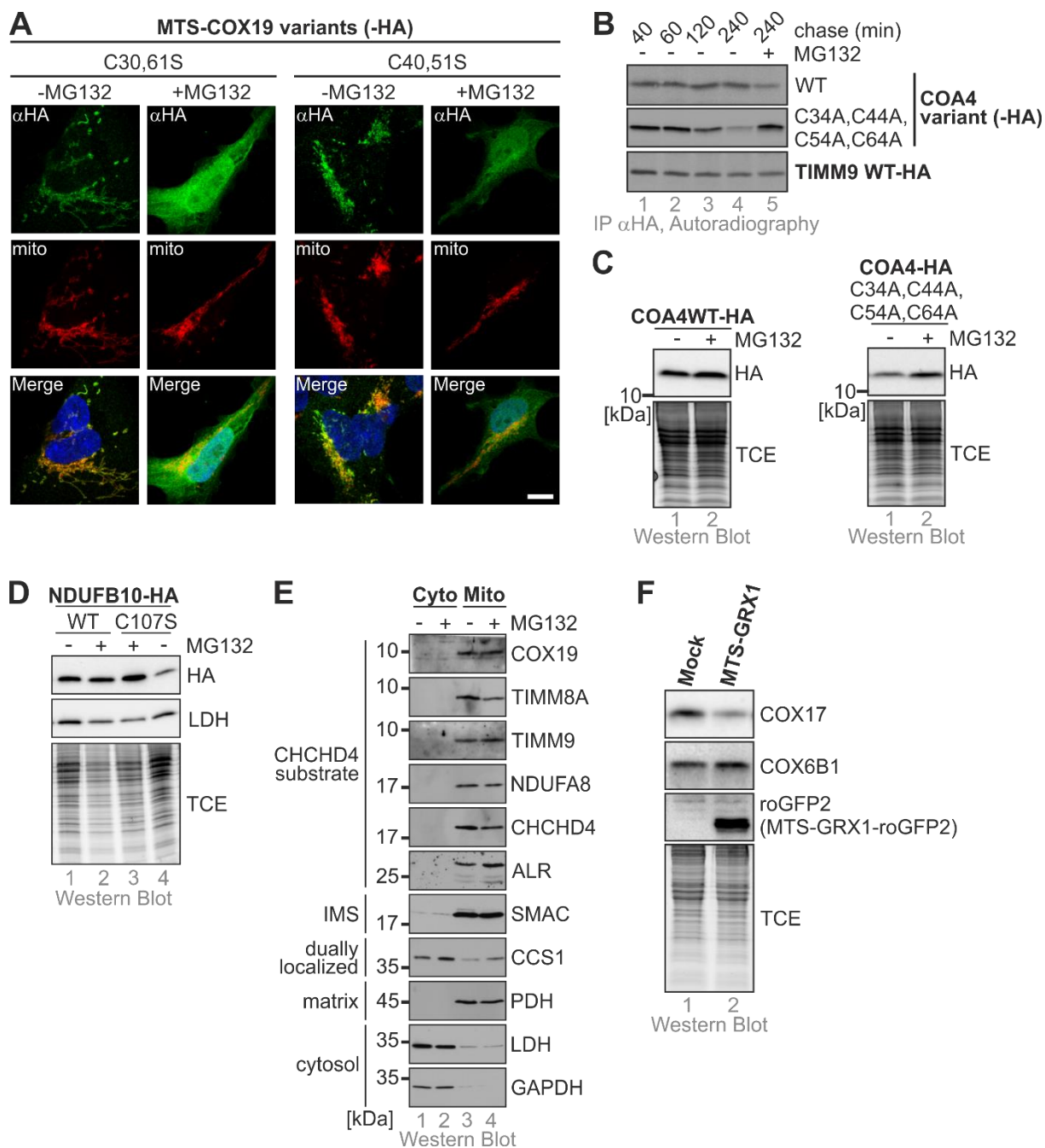
**A)** Steady state levels of CHCHD4 substrates in HEK293 cells stably expressing different F68E variants of CHCHD4. Expression of CHCHD4 variants was induced for 5 days in glucose-containing medium. Cells were lysed and protein levels were analysed by SDS-PAGE and immunoblot against the indicated proteins. CHCHD4<sup>F68E</sup> variants exhibit no deleterious effect for substrate levels. (n=2-3 biological replicates)

**B)** Quantification of (A) shows substrate-specific differences in substrate levels.

**C)** Viability of cells upon overexpression of CHCHD4 F68E variants. Expression of CHCHD4 variants was induced for 4 and 7 days in galactose-containing medium. Cells were analysed by PrestoBlue Cell Viability Reagent. CHCHD4<sup>F68E</sup> variants exhibit no deleterious effect on growth. Fold viability is presented as the viability data of induced cells divided by the data of non-induced cells of the same cell line. (n=3 biological replicates)

**D-F)** Only CHCHD4<sup>WT</sup> can oxidize COX19. Small amounts of *in vitro* translated radioactive COX19 were incubated with buffer for the indicated times, TCA-precipitated, and incubated with 15 mM mmPEG24 for 1 hr at 25°C. Protein was analysed by non-reducing SDS-PAGE and autoradiography. Reduced and oxidized forms of COX19 are indicated. (n=1)

**G)** Redox state of cysteine variants of CHCHD4. C53S and C55S are reduced at steady state. Performed as described in Figure **S3C**. This indicates that in thiol-disulphide-exchange reactions these variants would execute nucleophilic attacks. (n=2 biological replicates)



**Supplementary Figure 6. Proteasome and IMS redox influence CHCHD4 substrates.** (related to Figure 6)

**A)** Localization of MTS-COX19 cysteine variants in the presence and absence of proteasomal inhibitor. Experiment was performed as described in Figure 1E except that cells were cultured in the presence or absence of the proteasomal inhibitor MG132. Like the four-fold cysteine mutant of COX19 (Figure 6B), the mutants lacking the two cysteines required for formation of the inner or outer disulphide bonds, respectively accumulate in the cytosol upon MG132 treatment. MitoTrackerRed was used to stain mitochondria (mito). Scale bar = 10  $\mu$ m. (C30,61S: n=37, C40,51S: 27 cells, technical replicates)

**B)** Pulse chase stability assay of COA4 cysteine variants. Cysteine variants but not the wildtype are stabilized by MG132 treatment. Performed as described in Figure 6C. For proteasome inhibition 5  $\mu$ M MG132 was present throughout the pulse chase experiment. (n=2 biological replicates)

**C)** Steady state levels of COA4 wild type and cysteine variant. The COA4 cysteine variant is stabilized by MG132 treatment. For proteasome inhibition, cells were treated with 5  $\mu$ M MG132 for 4 h prior to cell lysis. (n=3 biological replicates)

**D)** Steady state levels of NDUFB10 wild type and cysteine variant (NDUFB10<sup>C107S</sup>). NDUFB10<sup>C107S</sup> is stabilized by MG132 treatment. For proteasome inhibition, cells were treated with 5  $\mu$ M MG132 for 4 h prior to cell lysis. (n=1)

**E)** Levels of endogenous CHCHD4 substrate proteins in HEK293 cells upon treatment with MG132. HEK293 cells were treated with 5  $\mu$ M MG132 for 4 h or remained untreated. Cells were fractionated and separated by centrifugation into mitochondrial and cytosolic fractions. Cellular fractions were separated by SDS-PAGE and analyzed by immunoblot using antibodies against the indicated proteins. (n=1)

**F)** Steady state levels of endogenous CHCHD4 substrates upon overexpression of IMS-localized GRX1. Expression of MTS-GRX1 was induced for 5 days in glucose-containing medium. Cells were lysed and protein levels were analysed by SDS-PAGE and immunoblot against the indicated proteins. Endogenous COX17 levels are decreased upon increased levels of IMS-localized GRX1. This is in line for a potential role of GRX1 in modulating import and oxidation of selected CHCHD4 substrates. (n=4 biological replicates)